H_∞ Bumpless Transfer Under Controller Uncertainty

Kai Zheng, Tamer Başar, and Joseph Bentsman

***Abstract*—The internal model-based H_∞ full information steady-state bumpless transfer synthesis procedure is developed and demonstrated to provide near optimal robust stability and robust performance for a much larger class of controller uncertainty than the earlier developed LQ state/output transfer. It is also pointed out that the steady-state bumpless transfer under controller uncertainty represents, in general, a hybrid mode of system behavior—a controlled discrete transition.**

***Index Terms*—Bumpless transfer, computational speedup, controller uncertainty, robust control.**

I. Introduction

Switching between two dynamic controllers that does not induce bumps in the plant output, referred to as bumpless transfer, arises in many cases of practical interest. One such case is switching between several linear controllers, each designed to provide the desired closed-loop performance in the neighborhood of its operating point, to cover the entire operating range of a nonlinear plant ([1]–[3]). Another case is the attainment of an improved closed-loop system performance via switching between the controllers with the complementary properties, such as the ones separately optimized for tracking and disturbance rejection ([4]). A third case is an online performance assessment of the advanced control laws against the industry standard ones in large industrial process control units ([5], [6]). In many of these cases, the controllers involved are multi-input-multi-output (MIMO) and of high order and implemented in software so that their states are available. Bumpless transfer is often performed in the steady state to meet safety requirements.

In the basic transfer setting shown in Fig. 1, controllers 1 and 2 are the online and the offline ones, respectively, and the transfer from 1 to 2 is contemplated. It is seen that bumpless transfer is achieved if and only if the values of the input and the output signals of the offline controller are, respectively, equal to those of the online one prior to controller transfer. In Fig. 1, e', u', α and u are the inputs and the outputs of the controllers 1 and 2, and r and y are the reference input and the plant output, respectively. In the steady state, all of the above signals are constant. If prior to transfer from controller 1 to 2 the equalities $\alpha = e'$, $u = u'$ are enforced by a transfer operator governing the off-line controller, then after transfer both the plant and the controller 2, being already in the steady state prior to transfer, will remain in the steady state.

Manuscript received December 06, 2008; revised March 20, 2009 and March 21, 2009. First published June 23, 2009; current version published July 09, 2009. This work has been supported by the National Science Foundation under Grants CMS-0324630, ECS-0501407, and DMI-0500453, by the Grainger Center for Electric Machinery and Electromechanics at UIUC, and by the Electric Power Research Institute. This work was presented in part at the Proceedings of the 46th IEEE CDCNew Orleans, LA, Dec.12–14, 2007. Recommended by Associate Editor Z. Wang.

K. Zheng was with the University of Illinois at Urbana-Champaign, Urbana IL 61801 USA. He is now with Arcelor Mittal Steel Company USA R&D, East Chicago, IL 46322 USA (e-mail: kai.zheng@arcelormittal.com).

T. Başar is with the Coordinated Science Laboratory and Electric and Computer Engineering Department, University of Illinois at Urbana-Champaign, Urbana IL 61801 USA (e-mail: basar1@illinois.edu).

J. Bentsman is with the Department of Mechanical Science and Engineering, University of Illinois at Urbana-Champaign, Urbana IL 61801 USA (e-mail: jbentsma@illinois.edu).

Digital Object Identifier 10.1109/TAC.2009.2020648

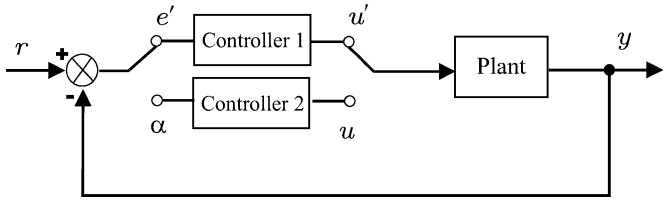

Fig. 1. Diagram illustrating bumpless transfer.

A closer look at applications reveals, however, that the above necessary and sufficient condition, and hence bumpless transfer, is not always achievable, the reason being the difference, in general, in the steady-state controller gains. Namely, if the steady-state gain of controller 2 in Fig. 1 differs from that of controller 1, it is impossible to achieve $\alpha = e'$, $u = u'$ simultaneously in the steady state. Due to this reason, in the majority of controller transfer applications, the transfer operator is designed to only ensure that the values of the output signals of the off-line controller are equal to those of the online one, which is also the approach taken in this technical note.

The classical results in bumpless transfer ([7], [8]) assume perfect knowledge of the implemented controller dynamics. However, controller uncertainty has been reported in a number of applications [5], [6]. Indeed, perfect implementation of, say, MATLAB designed linear H_∞ controller in real-time software/hardware could be impossible for a variety of reasons, such as software implementation error and hardware inadequacy, e.g. variable programmable logic controller (PLC) scan times [5]. Apart from that, the approximation error could be caused by undocumented and/or unavailable models of the existing controllers, especially those of the older legacy MIMO PID clusters nearing replacement, and the use of the linearized models to represent the nonlinear controllers in the linear transfer operator synthesis. As a result, in these applications there is a significant mismatch between the continuous-time linear controller models used in the bumpless transfer design and the actual controller dynamics. In the case of robust controller implementation, this mismatch, even a pronounced one, usually causes no problem in normal operation due to the inherent closed-loop robustness and goes unnoticed. The situation, however, drastically changes when controller transfer is needed. Then, the offline controller itself becomes the object of control, controller uncertainty precludes accessing the true offline controller state, and pronounced mismatch between the controller model and the true controller dynamics makes bumpless transfer a nontrivial problem. In these cases, the true off-line controller state is replaced in implementation by *the nominal state*, x_{nom}, of the off-line controller that can be viewed as the state of the controller model. Hence the use of only the nominal state x_{nom} of the controller along with its input can no longer provide its actual output, inducing bumps during controller transfer [6].

Based on this consideration, a complete design and implementation methodology for the steady-state bumpless controller transfer under controller uncertainty is presented in [6]. The state/output feedback topology proposed therein employs the nominal state of the offline controller and, through the use of an additional integral type controller/model mismatch compensator, also the actual offline controller output. [6] presents the supporting theory and establishes the applicability of the design procedure to a large class of systems with uncertainty types compatible with linear quadratic state feedback. This technique is briefly summarized next.

The state/output feedback topology proposed in [6] is shown in Fig. 2. The transfer operator in this topology is seen to combine two distinct transfer operators in a nested configuration: the inner one, F,

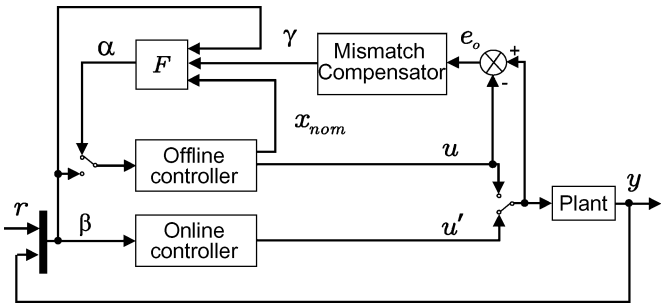

Fig. 2. State/output feedback bumpless transfer topology.

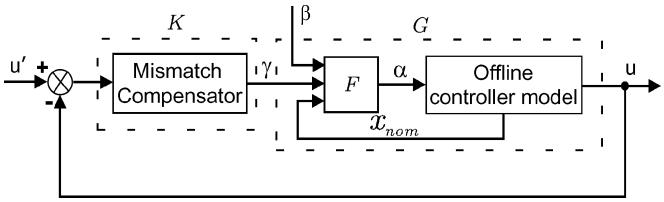

Fig. 3. Nominal offline controller subsystem in the state/output feedback topology.

and the outer one, the mismatch compensator, forming the state and the output feedback loops, respectively. The inner operator F is designed to stabilize the offline controller and the outer mismatch compensator then drives the offline controller output u to converge to the online controller output u'. After the attainment of the latter, the switch at the input side of the offline controller turns to connect signal β to the offline controller. At the same time, the switch at the offline controller output side turns to disconnect online controller output u' from the plant input and connect the offline controller output u to the plant input, completing the bumpless transfer. This configuration permits retaining the infinite horizon LQ design of [8] for the inner loop, while employing, under certain conditions, a simple integral control law for the outer loop. To demonstrate this, the offline controller subsystem in Fig. 2 with no offline controller uncertainty should be rearranged, as first observed in [6], into that shown in Fig. 3.

For the above topology, the LQ technique of [8] is extended in [6] to synthesis of the feedback matrix F to retain the robustness and the computational convenience of the full state LQ design. The matrix F is then obtained through a quadratic minimization of the functional J that includes the difference between two sets of signals, the input signals $\alpha(t)$ and $\beta(t)$ driving the controllers, and the off-line controller and the mismatch compensator outputs $u(t)$ and $\gamma(t)$, respectively, given by

$$J(u,\alpha)=\frac{1}{2}\int_0^\infty \left[z_u(t)^\top W_u z_u(t)+z_e(t)^\top W_e z_e(t)\right]dt \qquad (1)$$

where $z_u(t)=u(t)-\gamma(t)$, $z_e(t)=\alpha(t)-\beta(t)$, and W_u and W_e are constant positive definite weighting matrices of appropriate dimensions used to tune the design. The existence of the stabilizing state feedback matrix F is guaranteed for any controllable and observable offline controller state space realization. Controller K is shown to have decentralized structure $diag\{k_1/s,\ldots,k_n/s\}$.

The design approach proposed in [6] consists of two steps: 1) synthesis of the state feedback matrix F to stabilize the off-line controller under controller uncertainty and 2) design of the mismatch compensator to drive the output tracking error to zero. This approach, further referred to as the two-step approach, yields the transfer operators that meet the objectives indicated above with simple and transparent structures. Moreover, this approach has been rigorously shown in [9] to be applicable to a large class of controllers.

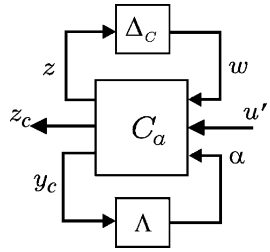

Fig. 4. General synthesis framework.

A drawback of this approach, however, is that it lacks a general characterization of the controller uncertainty under which the design objectives are achieved by a synthesized transfer operator. The LQ full state feedback synthesis exploited in this approach does not provide a unified framework, such as that of H_∞ synthesis, for rigorously characterizing more general types of uncertainty and robustness margins, directly incorporating them into the design procedure for achieving the optimal or suboptimal stability robustness, and specifying more general internal models for the transfer conditions.

Thus, it is of interest to investigate the capabilities of H_∞ synthesis in transfer operator design under controller uncertainty. This is carried out in the current work.

Notation: $\|A\|_2$ denotes the 2 norm of a matrix A. $\|B\|_\infty = \sup_{\omega\in R}\bar{\sigma}[B(j\omega)]$ denotes the H_∞ norm of a transfer function B.

II. Problem Formulation

First, let the offline controller model be realized by

$$\begin{aligned}\dot{x}&=Ax+B_2\alpha\\ u&=C_2x+D_{22}\alpha\end{aligned} \qquad (2)$$

where x, α and u, are the controller state, input, and output, respectively, and A, B_2, C_2, and D_{22} are matrices of appropriate dimensions. Under the H_∞ synthesis framework, the implemented offline controller can be represented as

$$\begin{aligned}\dot{x}&=Ax+B_1w+B_2\alpha,\\ z&=C_1x+D_{11}w+D_{12}\alpha\\ u&=C_2x+D_{21}w+D_{22}\alpha\end{aligned} \qquad (3)$$

where w and z are the uncertainty input and output, respectively, and B_1, C_1, D_{11}, D_{12}, and D_{21} are matrices of appropriate dimensions. Denote the uncertainty block linking w and z to be Δ_C such that $w=\Delta_C z$. This representation captures a variety of uncertainty types, including input and output multiplicative, input and output additive, and parametric. For example, to represent up to 20% parametric uncertainty in matrix A, i.e. to represent the following implemented controller:

$$\begin{aligned}\dot{x}&=(A+\Delta_A)x+B_2\alpha\\ u&=C_2x+D_{22}\alpha\end{aligned} \qquad (4)$$

where $(\|\Delta_A\|_2/\|A\|_2)<0.2$, simply let $C_1=I$, $D_{11}=D_{12}=D_{21}=0$, $B_1=0.2\|A\|_2 I$, Δ_C be unstructured, and $\|\Delta_C\|_\infty<1$.

With the above controller uncertainty representation, the general robust transfer operator synthesis diagram for bumpless transfer under controller uncertainty is depicted in Fig. 4, where C_a is the augmented off-line controller, z_C is the quantity to be made small, y_C is the output of the augmented controller available for the transfer operator Λ to be synthesized, and u' is the online controller output to be tracked by the off-line controller output u.

In the online operating context, the steady-state bumpless transfer under controller uncertainty represents a particular hybrid system event—a so-called controlled discrete transition [10]. Indeed, as seen, for example, in Fig. 2, the transfer operator acts only in the offline controller subsystem. The latter becomes decoupled from the online process dynamics as soon as the steady state (or its sufficiently small neighborhood) is reached. Upon decoupling, an instantaneous, in theory, convergence of the offline controller output to that of the online controller under the offline controller uncertainty is enforceable by the transfer operator through the infinite speedup of the offline closed loop computation ([1]), thus admitting instantaneous controller transfer.

Due to this feature, the robust transfer operator performance could be optimized not as tightly as the robust controller performance in a regular controller design. The stability and performance robustness of the bumpless transfer operator design can then be simply addressed in a small gain theorem setting using unstructured uncertainty, as discussed, for example, in [11, p. 3], by defining $\mathbf{v} = [z^\top \; z_C^\top]^\top$, $\mathbf{d} = [w^\top \; (u')^\top]^\top$, and Δ_P—the performance uncertainty such that $u' = \Delta_P z_C$, and carrying out the suboptimal H_∞ design of the transfer operator Λ that satisfies a given bound on the unstructured singular value $\|\mathbf{T_{vd}}\|_\infty$ of $\mathbf{T_{vd}}$, providing the structural transparency of the resulting design at the expense of conservativeness.

Thus, the objectives of the H_∞ suboptimal transfer operator synthesis for bumpless transfer under controller uncertainty are formulated as follows: 1) given $\gamma_s > 0$, find the transfer operator Λ such that $\|\mathbf{T_{vd}}\|_\infty < \gamma_s$, the system in Fig. 4 is stable for all stable $diag(\Delta_C, \Delta_P)$ satisfying $\|diag(\Delta_C, \Delta_P)\|_\infty < 1/\gamma_s$ and 2) $\lim_{t\to\infty} u(t) - u'(t) = 0$ with some nominal convergence rate. This synthesis is carried out in the next section.

III. H_∞ Full Information Internal Model-Based Steady-State Transfer Operator Synthesis

This section presents the main contribution of the technical note—the demonstration that the concept of the full information set for bumpless transfer under controller uncertainty introduced in [6] reduces the transfer operator design to the H_∞ full information controller synthesis problem [12] readily solvable by means of an algebraic Riccati equation. Robust stability and robust performance of bumpless transfer setting in Figs. 4 and 5 then come as a consequence of the application of the H_∞ full information synthesis and small gain theorem.

The key to address controller uncertainty in bumpless transfer is to exploit the full information set [6], which allows the maximum robustness to be achieved and at the same time forces the output of the off-line controller to converge to the online one. The full information set introduced in [6] consists of the online controller input and output, and the off-line controller state, input, and output. According to the internal model principle, to track a constant reference signal with zero steady-state tracking error, the loop transfer matrix must contain a model of the constant reference signal, which is simply an integrator. Thus, the state of the latter should also be included in the full information set. Since only tracking of the online controller output is achievable and is of interest [9], the online controller input does not contribute to the synthesis and hence can be left out. Thus, the full information set for the steady-state bumpless transfer under controller uncertainty in this case consists of the off-line controller state, input, and output, the augmenting integrator state, and the online controller output. Since the off-line controller state x, the off-line controller input α, and the uncertainty input w in (3) fully characterize the off-line controller output u, allowing the transfer operator to have access to the full information set is equivalent to providing to it the off-line controller state x, the augmenting integrator state, further referred to as γ, the uncertainty input

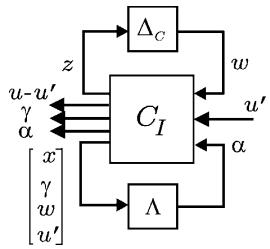

Fig. 5. LFT diagram for the internal model-based transfer operator synthesis.

w, and the online controller output u', i.e. y_C should be chosen to be $[x^\top \; \gamma^\top \; w^\top \; (u')^\top]^\top$. Since the off-line controller output u is required to track the online controller output u', it is natural to let the tracking error $u - u'$ be regulated. Finally, the output α of the transfer operator and the state γ of the integrator should be regulated as well to prevent them from being excessively large. Thus, the generalized off-line controller takes the following form:

$$\begin{aligned}
\dot{x} &= Ax + B_1 w + B_2 \alpha \\
\dot{\gamma} &= C_2 x + D_{21} w + D_{22} \alpha - u' \\
z &= C_1 x + D_{11} w + D_{12} \alpha \\
u - u' &= C_2 x + D_{21} w - u' + D_{22} \alpha \\
\gamma &= \gamma, \\
\alpha &= \alpha \\
y_c &= \begin{bmatrix} x^\top & \gamma & w^\top & (u')^\top \end{bmatrix}^\top .
\end{aligned} \tag{5}$$

The corresponding LFT diagram for synthesis is shown in Fig. 5. It is then clearly seen that finding a transfer operator Λ to stabilize the system in Fig. 5 and making $u - u'$ small constitutes essentially an H_∞ full information control problem [11], [12]. Solution of this problem given in [11], [12] is specialized to system (5) in the following theorem.

Theorem 1: Consider (5) rewritten as

$$\begin{aligned}
\dot{\mathbf{x}} &= \mathbf{A}\mathbf{x} + \mathbf{B}_1 \mathbf{d} + \mathbf{B}_2 \boldsymbol{\alpha}, \\
\mathbf{v} &= \mathbf{C}_1 \mathbf{x} + \mathbf{D}_{11} \mathbf{d} + \mathbf{D}_{12} \boldsymbol{\alpha}, \\
\mathbf{y}_c &= \mathbf{C}_2 \mathbf{x} + \mathbf{D}_{21} \mathbf{d} + \mathbf{D}_{22} \boldsymbol{\alpha}
\end{aligned} \tag{6}$$

where $\mathbf{x} = [x^\top \; \gamma^\top]^\top$, $\mathbf{v} = [z^\top \; (u - u')^\top \; \gamma^\top \; \alpha^\top]^\top$, $\mathbf{d} = [w^\top \; (u')^\top]^\top$, $\boldsymbol{\alpha} = \alpha$, $\mathbf{A} = \begin{bmatrix} A & 0 \\ C_2 & 0 \end{bmatrix}$, $\mathbf{B}_1 = \begin{bmatrix} B_1 & 0 \\ D_{21} & -I \end{bmatrix}$, $\mathbf{B}_2 = \begin{bmatrix} B_2 \\ D_{22} \end{bmatrix}$, $\mathbf{C}_1 = \begin{bmatrix} C_1^\top & C_2^\top & 0 & 0 \\ 0 & 0 & I & 0 \end{bmatrix}^\top$, $\mathbf{D}_{11} = \begin{bmatrix} D_{11}^\top & D_{12}^\top & 0 & 0 \\ 0 & -I & 0 & 0 \end{bmatrix}^\top$, $\mathbf{D}_{12} = [D_{12}^\top \; D_{22}^\top \; 0 \; I]^\top$, $\mathbf{C}_2 = \begin{bmatrix} I & 0 & 0 & 0 \\ 0 & I & 0 & 0 \end{bmatrix}^\top$, $\mathbf{D}_{21} = \begin{bmatrix} 0 & 0 & I & 0 \\ 0 & 0 & 0 & I \end{bmatrix}^\top$, $\mathbf{D}_{22} = 0$. Denote further $\mathbf{B} = [\mathbf{B}_1 \; \mathbf{B}_2]$, $\mathbf{D}_1 = [\mathbf{D}_{11} \; \mathbf{D}_{12}]$, $R = D_1^\top D_1 - \begin{bmatrix} \gamma_s^2 I_{m_1} & 0 \\ 0 & 0 \end{bmatrix}$, where m_1 is the dimension of $\mathbf{d}$ and let $\mathbf{T_{vd}}$ be the transfer function from $\mathbf{d}$ to $\mathbf{v}$.

Suppose the following assumptions are satisfied:

1) $(\mathbf{A}, \mathbf{B}_2)$ is stabilizable;
2) there is a matrix $\mathbf{D}_\perp$ such that $[\mathbf{D}_{12} \; \mathbf{D}_\perp]$ is unitary;
3) $\begin{bmatrix} \mathbf{A} - j\omega I & \mathbf{B}_2 \\ \mathbf{C}_1 & \mathbf{D}_{12} \end{bmatrix}$ has full column rank for all ω.

Then, an H_∞ suboptimal transfer operator Λ satisfying $\|\mathbf{T_{vd}}\|_\infty < \gamma_s$ and guaranteeing stability for $\|diag(\Delta_C, \Delta_P)\|_\infty < 1/\gamma_s$ is given by

$$\alpha = -\mathbf{D}_{12}^\top \mathbf{D}_{11} \begin{bmatrix} w \\ u' \end{bmatrix} + \begin{bmatrix} \mathbf{D}_{12}^\top \mathbf{D}_{11} & I \end{bmatrix} F \mathbf{x} \tag{7}$$

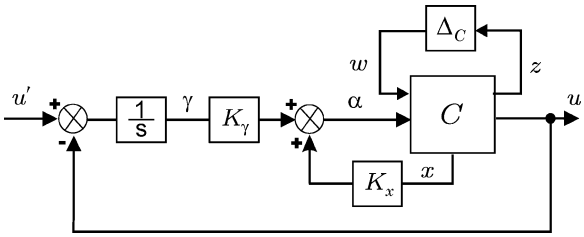

Fig. 6. Internal model-based H_∞ transfer topology.

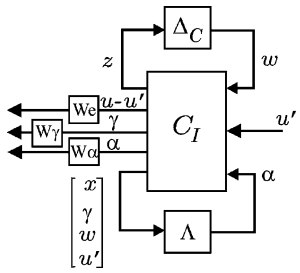

Fig. 7. Weighted LFT diagram for the internal model-based transfer operator synthesis.

where

$$F = -R^{-1}\left[\mathbf{D}_1^\top \mathbf{C}_1 + \mathbf{B}^\top X_\infty\right] \tag{8}$$

and X_∞ is the positive semi-definite solution of the ARE

$$\left(\mathbf{A} - \mathbf{B}R^{-1}\mathbf{D}_1^\top \mathbf{C}_1\right)^\top X_\infty + X_\infty\left(\mathbf{A} - \mathbf{B}R^{-1}\mathbf{D}_1^\top \mathbf{C}_1\right) - X_\infty \mathbf{B}R^{-1}\mathbf{B}^\top X_\infty + \mathbf{C}_1^\top \mathbf{C}_1 - \mathbf{C}_1^\top \mathbf{D}_1 \mathbf{R}^{-1}\mathbf{D}_1^\top \mathbf{C}_1 = 0$$

assuming such X_∞ exists and $\sigma(\mathbf{D}_\perp^\top \mathbf{D}_{11}) < \gamma_s$.

Proof: Directly follows from Theorems 16.9 and 17.6 (a) in [11] and a small gain theorem. ■

Assumption 2, leading to $\mathbf{D}_{22} = 0$, can be relaxed (cf. the footnote in [13, p. 291]).

From (7), it can be seen that the suboptimal transfer operator consists of a state feedback controller, an uncertainty input feedback controller, and a reference input feedback controller, all of which are static. Moreover, if the uncertainty input and the controlled input components in the regulated output, $\mathbf{v}$, are orthogonal to each other, i.e. $\mathbf{D}_{12}^\top \mathbf{D}_{11} = 0$, then (7) can be simplified to $\alpha = [0\ I]F\mathbf{x}$, namely, the suboptimal transfer operator in this case is simply a state feedback one. Enforcing the latter condition without loss of generality, the suboptimal transfer operator becomes $\alpha = K_x x + K_\gamma \gamma$ where K_x and K_γ are constant matrices of appropriate dimensions and

$$[K_x \quad K_\gamma] = [0 \quad I]F. \tag{9}$$

It is then seen that the resulting transfer operator has the same structure as the one designed by the two-step approach (cf. Fig. 2), i.e. both operators consist of a static state feedback controller in the inner loop and a simple integral mismatch compensator in the outer loop, as shown in Fig. 6.

IV. Robust Transfer Operator Synthesis Techniques

The purpose of this section is to show how the internal model-based H_∞ full information transfer synthesis procedure, further referred to as the H_∞ technique, proposed in this technical note, could be organized, provide a specific example of the application of this technique, and, using this example, compare the technique with the two-step approach introduced in [6].

In the example considered, the three-input-three-output tracking controller of [4] with the state dimension 8 is used as the offline controller to which the transfer operators obtained through these two techniques are applied. After model reduction, the state dimension reduces to 4. A realization of the final design is given by (2), where

$$A = \begin{bmatrix} -0.1003 & 0.0004 & 0 & -0.3261 \\ -0.0004 & -0.1003 & 0 & -1.8537 \\ 0 & 0 & -0.0010 & 0 \\ -1.8797 & 0.0925 & 0 & -1998.3 \end{bmatrix}$$

$$B_2 = \begin{bmatrix} 18.2 & -335.0 & 0 \\ 335.0 & 18.2 & 0 \\ 0 & 0 & -3.5 \\ 29.9 & -3148.9 & 0 \end{bmatrix}$$

$$C_2 = \begin{bmatrix} -334.2 & 30.2 & 0 & -278.3 \\ -30.2 & -334.1 & 0 & -3136.7 \\ 0 & 0 & -3.5 & 0 \end{bmatrix}$$

and $D_{22} = 0$.

The following scenario is adopted for the purpose of the comparison: design two transfer operators by the two-step approach and the H_∞ technique, respectively, to satisfy the objectives set forth in this technical note with a convergence time of 0.1 s. The resulting transfer operators will be referred to as the two-step design and the H_∞ design, respectively. Then, compare the stability robustness of the off-line controller subsystems under these two designs with respect to parametric uncertainty in the A matrix, and also performance robustness. This implies that the implemented tracking controller takes the form of (4).

A. The H_∞ Design

As discussed in Section II, choose $C_1 = I, D_{11} = D_{12} = D_{21} = 0$, $B_1 = I$ and augment the tracking controller model as (5). To enable the trade-off between the time-domain nominal performance and robustness, the generalized offline controller C_I in Fig. 5 is further augmented with three constant weighting matrices W_e, W_γ, W_α, as shown in Fig. 7. Thus, the regulated output becomes $\mathbf{v} = [z^\top\ [W_e(u-u')]^\top\ [W_\gamma \gamma]^\top\ [W_\alpha \alpha]^\top]^\top$. It then follows that the state-space realization of the system in Fig. 7 can be given by (6) with matrices $\mathbf{A}, \mathbf{B}_1, \mathbf{B}_2, \mathbf{C}_2, \mathbf{D}_{21}, \mathbf{D}_{22}$ given in the previous section, and $\mathbf{C}_1, \mathbf{D}_{11}, \mathbf{D}_{12}$ given by $\mathbf{C}_1 = \begin{bmatrix} C_1 & 0 \\ W_e C_2 & 0 \\ 0 & W_\gamma I \\ 0 & 0 \end{bmatrix}$, $\mathbf{D}_{11} = \begin{bmatrix} D_{11} & 0 \\ D_{12} & -W_e \\ 0 & 0 \\ 0 & 0 \end{bmatrix}$, and $\mathbf{D}_{12} = [D_{12}^\top\ D_{22}^\top\ 0\ W_u^\top]^\top$. (9) can then be used to compute suboptimal transfer operators for a given combination of γ_s, W_e, W_γ, and W_u. The following steps are adopted in reaching a successful design.

1) Select W_e, W_γ, and W_u.
2) Carry out a bisection iteration on γ_s (cf. [13]) to find a γ_s that produces $X_\infty \geq 0$ and $\sigma(\mathbf{D}_\perp^* \mathbf{D}_{11}) < \gamma_s$, and $\gamma_s - \gamma_{opt} < tol$, where γ_{opt} is the smallest possible γ_s that yields $X_\infty \geq 0$ and $\sigma(\mathbf{D}_\perp^* \mathbf{D}_{11}) < \gamma_s$, and tol denotes the error tolerance.
3) Check the time domain nominal performance of the off-line controller subsystem. If a convergence time of 0.1 s is achieved, stop. Otherwise, change W_e, W_γ, and W_u and go back to step 2.

After several iterations, the weighting matrices are chosen to be $W_e = diag\{0.06, 0.06, 0.01\}$, $W_\gamma = diag\{5, 5, 600\}$, and $W_u = diag\{0.01, 0.01, 0.5\}$, for which $\gamma_{1s} = \|\mathbf{T_{1vd}}\|_\infty = 5.003$. The H_∞ norm of the transfer function from the uncertainty input w to the uncertainty output z, $\|T_{1zw}\|_\infty$, is computed to be $\|T_{1zw}\|_\infty = 0.0447$. The resulting feedback matrices (cf. Fig. 6) are

$$K_x = \begin{bmatrix} 2009.3 & -439.9 & 0.0005 & -607.56 \\ 433.02 & 1967.7 & 0 & 18884 \\ 0.0001 & 0 & 1148.9 & 0 \end{bmatrix}$$

and

$$K_\gamma = \begin{bmatrix} -496.0695 & 62.8720 & -0.0188 \\ -62.8718 & -496.0677 & -0.0010 \\ 0 & 0 & -39227 \end{bmatrix}$$

yielding good nominal performance with no overshoot and convergence time of less than 0.1 s.

B. The Two-Step Design

First, weighting matrices W_e and W_u in the performance index (1) are chosen to be $diag\{9 \times 10^{-6}, 1.5 \times 10^{-6}, 60\}$, and $diag\{1, 1, 1\}$, respectively, yielding a 3×10 state feedback matrix F (cf. Fig. 2) that provides a convergence time of approximately 0.06 sec. Then, the target loop bandwidth is chosen to be 50 Hz for all three output channels and the convex optimization proposed in [6] is utilized to obtain the parameters of the mismatch compensator K as $k_1 = 30.2063$, $k_2 = 77.0649$, and $k_3 = 29.6241$. No design iteration is necessary. Simulation shows performance similar to that of the H_∞ design.

C. Robustness Comparison

It is easily seen that the two-step approach does not provide explicit robustness margin guarantees in terms of parametric uncertainty in matrix A. However, as discussed before, since the two-step design has the same structure as the H_∞ design, the LFT diagram in Fig. 7 can also be used to analyze the stability and performance robustness of the two-step design. Thus, inserting F and K obtained in the two-step design into the configuration in Fig. 7 and computing the H_∞ norm of the transfer function from the generalized external input $\mathbf{d}$ to the regulated output $\mathbf{v}$ yields

$$\gamma_{2s} = \|\mathbf{T_{2vd}}\|_\infty = 20.3. \tag{10}$$

The H_∞ norm of the transfer function from the uncertainty input w to the uncertainty output z, $\|T_{2zw}\|_\infty$, is

$$\|T_{2zw}\|_\infty = 0.0576. \tag{11}$$

It is then seen from comparing (11) with $\|T_{1zw}\|_\infty = 0.0447$ that $\|T_{2zw}\|_\infty$ achieved by the two-step design only slightly exceeds $\|T_{1zw}\|_\infty$ achieved by the H_∞ design, implying that near optimal stability is achieved by the former design. Moreover, it follows that the two-step design guarantees the offline controller subsystem to be stable under all parametric uncertainty ΔA in A such that

$$\|\Delta A\|_2 < \frac{1}{\|T_{2zw}\|_\infty} = 17.36 \tag{12}$$

whereas the H_∞ design provides slightly larger robustness margin

$$\|\Delta A\|_2 < \frac{1}{\|T_{1zw}\|_\infty} = 22.37. \tag{13}$$

Noticing that $\gamma_{2s} = \|\mathbf{T_{2vd}}\|_\infty = 20.3$ in (10) is much greater than $\gamma_{1s} = \|\mathbf{T_{1vd}}\|_\infty = 5.003$, on the other hand, reveals that the performance robustness of the two-step design is nowhere near optimal. To illustrate this, an uncertainty matrix ΔA_2 is generated by a random number generator with $\|\Delta A_2\|_2 = 15.62 = 17.36 \cdot 0.9$, i.e. the size of the uncertainty is 90% of the robustness margin shown in (12). The performance of the two-step design under this uncertainty is shown in Fig. 8, where it is clearly seen that although stability and convergence are both preserved, large overshoots and undershoots occur and the convergence time increases to about 0.2 s. Similarly, with another uncertainty matrix with uncertainty being 90% of the robustness margin shown in (13), the H_∞ design performance is almost unchanged, with both stability and performance well preserved.

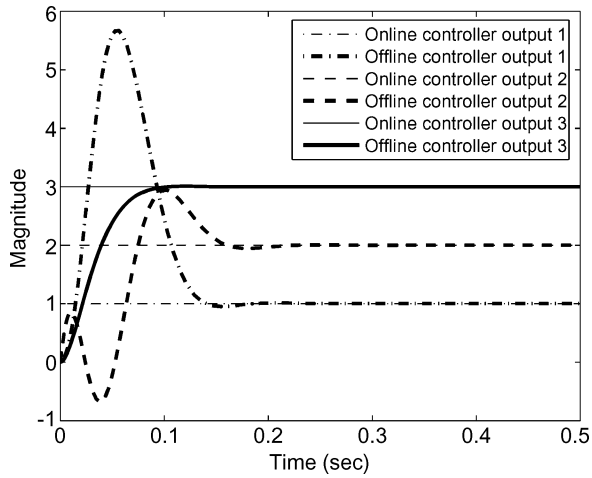

Fig. 8. Robust performance of the transfer operator designed using the two-step procedure.

The above comparison shows that, although with no *a priori* robustness guarantee, the two-step approach inherits the full state LQR near optimal stability robustness as well as its ease and transparency of design, whereas the H_∞ technique, by directly incorporating controller uncertainty, yields guaranteed essentially optimal stability robustness and suboptimal performance robustness for a large variety of controller uncertainty types, as seen in Fig. 7, but at the expense of a more complicated and less transparent design procedure.

V. Conclusion

The H_∞ steady-state bumpless transfer operator synthesis technique is developed that admits consistent incorporation of controller uncertainty. This is accomplished through the use of the full information set, as defined in [6], in the controller transfer that permits recasting the problem at hand into the H_∞ full information control problem setting. It is shown that under minimal loss of generality the resulting H_∞ transfer operator has the same structure as that designed by the two-step approach presented in [6], but provides an *a priori* guarantee of robust stability and robust performance.

References

[1] K. Zheng, J. Bentsman, and C. W. Taft, "Full operating range robust hybrid control of a coal-fired boiler/turbine unit," *ASME J. Dynam. Syst., Meas., Control*, vol. 130, no. 4, pp. 041 011-1–041 011-14, 2008.

[2] M. Turner, N. Aouf, D. G. Bates, I. Postlethwaite, and B. Boulet, "A switching scheme for full-envelope control of a V/STOL aircraft using LQ bumpless transfer," in *Proc. 2002 IEEE Int. Conf. Control Applications*, Glasgow, Scotland, U.K., Sep. 2002, pp. 120–125.

[3] J. D. Bendtsen, J. Stoustrup, and K. Trangbak, "Bumpless transfer between advanced controllers with applications to power plant control," in *Proc. 42nd IEEE Conf. Decision and Control*, Maui, HI, Dec. 2003, pp. 2059–2064.

[4] K. Zheng, A.-H. Lee, J. Bentsman, and P. T. Krein, "High performance robust linear controller synthesis for an induction motor using a multi-objective hybrid control strategy," *Nonlin. Anal.*, vol. 65, pp. 2061–2081, 2006.

[5] S. F. Graebe and A. L. B. Ahlen, "Dynamic transfer among alternate controllers and its relation to anti-windup controller design," *IEEE Trans. Control Syst. Technol.*, vol. 4, no. 1, pp. 92–99, Jan. 1996.
[6] K. Zheng, A.-H. Lee, J. Bentsman, and C. W. Taft, "Steady-state bumpless transfer under controller uncertainty using the state/output feedback topology," *IEEE Trans. Control Systems Technol.*, vol. 14, no. 1, pp. 3–17, Jan. 2006.
[7] M. Kothare, P. Campo, M. Morari, and C. Nett, "A unified framework for the study of anti-windup designs," *Automatica*, vol. 30, no. 12, pp. 1869–1883, 1994.
[8] M. C. Turner and D. J. Walker, "Linear quadratic bumpless transfer," *Automatica*, vol. 36, pp. 1089–1101, Aug. 2000.
[9] K. Zheng and J. Bentsman, "Decentralized compensation of controller uncertainty in the steady-state bumpless transfer under the state/output feedback," *Int. J. Robust Nonlin. Control*, 2009, to appear.
[10] J. Bentsman, B. M. Miller, E. Y. Rubinovich, and K. Zheng, "Hybrid dynamical systems with controlled discrete transitions," *Nonlin. Anal.: Hybrid Syst. and Applic.*, vol. 1, no. 4, pp. 466–481, 2007.
[11] K. Zhou, J. Doyle, and K. Glover, *Robust and Optimal Control*. Upper Saddle River, NJ: Prentice-Hall, 1996.
[12] J. C. Doyle, K. Glover, P. P. Khargonekar, and B. A. Francis, "State-space solutions to standard H_2 and H_∞ problems," *IEEE Trans. Automat. Control*, vol. 34, no. 8, pp. 831–847, Aug. 1989.
[13] K. Zhou and J. Doyle, *Essentials of Robust Control*. Upper Saddle River, NJ: Prentice-Hall, 1998.

State Convergence of Passive Nonlinear Systems With an L^2 Input

Bayu Jayawardhana, *Member, IEEE*, and George Weiss

***Abstract*—We show that the state of a strictly output passive system with an L^2 input converges to zero. The result is applied to the disturbance rejection problem (with reference signal zero), where the disturbance can be decomposed into a finite superposition of sine waves of arbitrary but known frequencies and an L^2 signal. Using an LTI controller, constructed based on the internal model principle, the state trajectories of the plant (and hence also the error signal) converge to zero.**

***Index Terms*—Disturbance rejection problem, internal model principle, invariant sets under a semiflow, passive system.**

I. Introduction

Passive systems have a $\mathcal{C}^1$ storage function H (defined on the state space) which has the intuitive meaning of stored energy. The input signal u and the output signal y take values in the same inner product space. We denote the state of the system at time t by $x(t)$. The defining property of a passive system is that

$$\dot{H} \leq \langle y, u \rangle, \quad \text{where} \quad \dot{H} = \frac{\partial H(x)}{\partial x}\dot{x}. \tag{1}$$

The function H is often used as a Lyapunov function for analyzing the system stability. Many physical systems (electrical circuits, mechanical systems, etc.) are passive if the input and output variables are chosen carefully such that their product represents the flow of power into the system.

For passive nonlinear systems, various passivity-based control techniques have been proposed to achieve asymptotic stabilization of an equilibrium point, see for example Ortega *et al.* [7]–[9] and van der Schaft [11]. These stabilization methods exploit the proposition that the asymptotic stability of an equilibrium point can be established for a class of strictly output passive nonlinear systems with an additional detectability hypothesis and without input [11]. This, however, cannot be used to show the robustness property of the closed-loop system when an external bounded-energy disturbance signal is added to the input.

The convergence of the state trajectory x of a nonlinear plant $\mathbf{P}$ given an input signal u converging to zero has been studied by Sontag in [13]. Suppose that 0 is a globally asymptotically stable (GAS) equilibrium point of $\mathbf{P}$. It is shown in [13] that if for an input u with $u(t) \to 0$ and for an initial state $x(0)$, there exists a unique solution $x(t)$ of

$$\dot{x} = f(x, u) \tag{2}$$

defined for all $t \geq 0$ and x is bounded, then $x(t) \to 0$ as $t \to \infty$. This result has been generalized in Ryan [10] for L^p inputs, using the same assumption on the global asymptotic stability of the origin and assuming that f from (2) is such that $f(\cdot, 0)$ is locally Lipschitz and for every compact set $K \in \mathbb{R}^n$ there exists $c > 0$ such that

$$\|f(x, u) - f(x, 0)\| \leq c\|u\| \qquad \forall u \in \mathbb{R}^m, x \in K. \tag{3}$$

It is shown in [10] that if for a $u \in L^p(\mathbb{R}_+)$ and an initial state $x(0)$, there exists a state trajectory x defined for all $t \geq 0$ and x is bounded, then $x(t) \to 0$ as $t \to \infty$.

For a special class of systems, namely, strictly output passive and zero-state detectable systems (the precise definitions will be given in Section II), we derive a result related to those in [10] and [13]. In Section III, we use a technique from infinite-dimensional linear system theory to show that for any L^2 input there exists a unique state trajectory x defined for all $t \geq 0$ and $x(t) \to 0$ as $t \to \infty$. Here, we allow the function f from (2) to satisfy a weaker condition than (3), but we require in addition a local Lipschitz continuity type assumption. Our conclusion is stronger in the sense that we prove the existence of global solutions, instead of assuming it. A related result in Teel [14] says that if f from (2) is affine to the input u, $\mathbf{P}$ is dissipative with the supply rate $-\alpha(x) + \|u\|^p$ where $p \in [1, \infty)$, α is a positive function and $u \in L^p(\mathbb{R}_+)$, then the state trajectory x is bounded and $\alpha(x(t))$ tends to zero.

In Section IV, the main result is applied to solve the input disturbance rejection problem for passive nonlinear plants, where the disturbance can be decomposed into a finite superposition of sine waves of arbitrary but known frequencies and an L^2 signal. It is shown that if the plant is zero-state detectable and the storage function is proper (these concepts are defined in Section II), then using the classical internal model-based LTI controller, the state trajectories of the plant converge to zero.

II. Preliminaries

Notation: Throughout this technical note, the inner product on any Hilbert space is denoted by $\langle \cdot, \cdot \rangle$ and $\mathbb{R}_+ = [0, \infty)$. We refer to Khalil [4] and to [11] for basic concepts on nonlinear systems and on passivity theory. For a finite-dimensional vector x, we use the norm $\|x\| = (\sum_j |x_j|^2)^{1/2}$ and for matrices, we use the operator norm induced by $\|\cdot\|$ (the largest singular value). For any $\epsilon \geq 0$, we denote $\mathbf{B}_\epsilon = \{x \in \mathbb{R}^n \,|\, \|x\| \leq \epsilon\}$. For a square matrix A, $\sigma(A)$ denotes the set of its eigenvalues. For any finite-dimensional vector space $\mathcal{V}$ endowed

Manuscript received August 13, 2008. First published June 23, 2009; current version published July 09, 2009. Recommended by Associate Editor K. Fujimoto.

B. Jayawardhana is with the Faculty of Mathematics and Natural Sciences, University of Groningen, Gronigen, The Netherlands (e-mail: bayujw@ieee.org).

G. Weiss is with Department of Electrical Engineering-Systems, Tel Aviv University, Ramat Aviv 69978, Israel (e-mail: gweiss@eng.tau.ac.il).

Digital Object Identifier 10.1109/TAC.2009.2020661